Molecular Immunology 109 (2019) 149–156

Contents lists available at ScienceDirect

Molecular Immunology

journal homepage: www.elsevier.com/locate/molimm

A tetravalent single chain diabody (CD40/HER2) efficiently inhibits tumor proliferation through recruitment of T cells and anti-HER2 functions

Li Lu[a,1], Ningbo Liu[b,1], Kaihu Fan[a], Guojing Zhang[a], Chuan Li[a], Yongjia Yan[a], Tong Liu[a], Wei-Huahua Fu[a,*]

[a] Tianjin Medical University General Hospital, No. 154 Anshan Road, Heping District, Tianjin 300052, China
[b] Department of Oncology Surgery, The first hospital of Handan, Hebei province China

ARTICLE INFO

Keywords:
CD40
HER2
Cancer immunity
Single chain diabody
T cells

ABSTRACT

Our aim was to construct a CD40 × HER2 single chain diabody (ScDb) and determine its tumor-specific immune activation and anti-HER2 function. Overlap extension-polymerase chain reaction was applied in the construction of ScDb, and the protein was expressed with the pET28a (+)-Rosetta prokaryotic expression system. Soluble ScDb was purified by a nickel-nitrilotriacetic acid column. Dendritic cells (DC) was stimulated by ScDb and inhibited 4T1 cells proliferation in vitro. In 4T1 tumor mice model, lymphocyte infiltration was prominently detected in ScDb group, Caspase-3 expression was significantly upregulated. ScDb was labeled using quantum dots. Immunofluorescence assay indicated ScDb exhibited high affinity to HER2. T6-17 cells were inhibited by ScDb in vitro. The phosphorylation and expression levels of AKT, ERK were markedly decreased. In T6-17 tumor mice model. Compared to CD40 ScFv, HER2 ScFv and normal saline groups, tumor volume diminished significantly in ScDb group, and tumor cells showed extensive deformation, and pervasive karyopyknosis and karyorrhexis were found. In the present study, we successfully constructed a ScDb fragment and expressed it using a prokaryotic expression system. The in vivo and in vitro experimental results indicated that ScDb could inhibit the proliferation of tumor cells by stimulating the tumor-specific immunoreaction and blocking the HER2-related signaling pathway.

1. Introduction

Human Epidermal Receptor 2 (HER2), a member of the epidermal growth factor family, is overexpressed in epithelial-derived tumors (Slamon et al., 1987). Studies have shown that the expression of HER2 in gastric cancer tends to predict poor prognosis and a high degree of malignancy (Begnami et al., 2011). Targeting HER2 by blocking HER2-dependent activation of the PI3K/Akt and MAPK/ERK1/2 pathways (Yokoyama et al., 2006) has resulted in tumor growth inhibition in vivo. Therefore, HER2 has emerged as a promising target for antibody therapies. Trastuzumab can specifically bind to HER2 and block the activation of its downstream signaling pathways, which exert a significant effect in HER2-overexpressing breast and gastric cancers (Bang et al., 2010). However, drug resistance has hampered the long-term efficacy of targeted therapy, leading to an urgent need for more modifications and combinations of targeted therapy.

A revolution in cancer immunotherapy has recently emerged with the development of novel immunomodulatory antibodies, classified as immunostimulatory agonist monoclonal antibodies (mAbs) or checkpoint blocking mAbs. CD40/CD40L, as an important costimulatory pathway, mediates a broad spectrum of systemic immune processes, including T cell-dependent humoral responses (Kawashita et al., 2014). Malignant tumors were shown to inhibit the expression of CD40L on T lymphocytes, leading to arrest of antigen-presenting cells (APCs) and contributing to tumor immune escape (Yang et al., 2013). SGN-40 is an agonistic anti-CD40 mAb that has been used in the treatment of various hematological and lymphoid tumors (Chawla et al., 2013). However, mAbs have a high molecular weight and poor tissue penetration. To achieve a satisfactory therapeutic concentration, drugs must maintain a high plasma concentration, and the high metabolic burden of the liver and kidneys that accompanies treatment should not be ignored (Singer et al., 2008). Therefore, it is particularly important to rationally modify the antibody structure and develop multiple functional antibodies.

Recently, recombinant antibody (RAb) technology has provided an alternative approach for engineering low-cost antibodies with desirable affinities and specificities (Yau et al., 2003; Kramer and Hock, 2003).

* Corresponding author.
E-mail address: tjmughgs_fwh@163.com (W.-H. Fu).
[1] These authors contributed equally to this work, thus they are co-first author.

https://doi.org/10.1016/j.molimm.2019.03.001
Received 22 December 2018; Received in revised form 27 February 2019; Accepted 1 March 2019
Available online 02 April 2019

Bispecific antibodies (BsAbs), which are capable of simultaneous binding to two different targets, could overcome many defects of mAb therapies (Schrama et al., 2006). Bispecificity can be used in cancer immunotherapy to crosslink tumor cells to immune cells, such as cytotoxic T cells. This crosslinking accelerates the disruption of tumor cells by immune cells, which could improve antitumor therapy efficiency and lower costs by decreasing the doses needed for therapy (Cao, 2003; Kufer et al., 2004). In our previous research, a high-affinity CD40 single-chain antibody clone was screened, and its function was verified. In this study, we used gene recombination technology to splice CD40 single-chain antibody clones and HER2 single-chain antibody clones to obtain an anti-CD40 × HER2 single chain diabody (ScDb). The HER2 targeting function and immune activation function of this molecule were verified both in vitro and in vivo.

2. Materials and methods

2.1. Animals and cell lines

Female BALB/c (H2-d) and BALB/c-nude mice (6–8 weeks old; 25–30 g weight) were purchased from the Animal Resource Center at the Institute of Radioactive Medicine, Chinese Academy of Medical Sciences (Tianjin, China). Mice were housed in a pathogen-free room with free access to autoclaved food and fresh water. All experimental protocols were reviewed and approved by the Institutional Animal Care and Use Committee of Tianjin Medical University. T6-17 cells were given as a gift from Professor Hongtao Zhang (University of Pennsylvania, Pennsylvania, USA), and 4T1 cells were obtained from the American Type Culture Collection (ATCC, Rockville, MD) and cultured under the recommended conditions.

2.2. Cloning of variable (V) immunoglobulin domains

In our previous research, the high-affinity CD40 ScFv clone was screened by phage display and was applied as the template in the variable light-chain (VL) and V heavy-chain (VH) domains polymerase chain reaction (PCR). The recombinant pUC57 vector encoding HER2-ScFv was gifted by Professor Hongtao Zhang (University of Pennsylvania, USA) and was also used as the template for HER2 VH and VL amplification.

2.3. Construction of CD40 × HER2 ScDb and structural analysis

The CD40 × HER2 ScDb fragment was constructed by overlapped extension PCR (SOE-PCR). Six primers (Table 1) for PCR were designed based on the ScDb sequences. Here, ScDb was mainly constructed by three SOE-PCR steps: (i) Amplifying VH and VL: the CD40VH and CD40VL domains were PCR-amplified with primers P1–P4, and HER2 ScFv was PCR-amplified with primers P5–P6. (ii) Splicing HER2 ScFv and CD40VL with a flexible linker (Gly4Ser): HER2 ScFv-CD40VL was PCR-amplified with primers P4 and P5. (iii) Amplifying the ScDb gene: ScDb was PCR-amplified with primers P1 and P4 using the HER2 ScFv-CD40VL and CD40VH conformations described above (Fig. 5).

After purifying the ScDb genes, we introduced a *NdeI* site at the C-terminus and a *SalI* site at the N-terminus and C-terminus with primers P1 and P4, respectively. Finally, the full-length ScDb fragments were separated and purified by 1% (w/v) agarose gel electrophoresis. Then, the synthesized ScDb gene was cloned into the pET28a (+)vector using the introduced *NdeI* and *SalI* sites and transformed into *Escherichia coli* DH5α. The transformants were selected on Luria Bertani (LB) plates supplemented with 50 mg/L kanamycin and incubated overnight at 37 ℃. The kanamycin-positive clones were identified by PCR, and plasmids were extracted and analyzed by restriction enzyme digestion and electrophoresis. The plasmids containing the fragments of right sizes were confirmed by DNA sequencing. The protein tertiary structure was imitated by I-TASSER online.

2.4. Expression and purification of CD40 × HER2 ScDb

To express the bispecific diabody, we transformed the plasmid pET28a (+)-ScDb into E. coli Rosetta (DE3) (Invitrogen). *E. coli* cells containing the recombinant plasmids were inoculated into 15 mL of LB medium containing 50 mg/L kanamycin. Overnight cultures were transferred to 300 mL of fresh medium and were grown at 37℃ until they reached an A600 = 0.8. Isopropyl-b-D-thiogalactopyranoside (IPTG) was added to final concentrations of 0.1 mmol/L, 0.2 mmol/L, 0.5 mmol/L, and 1 mmol/L, and the cultures were further grown overnight at 37℃ for 4 h. *E. coli* cells were collected by centrifugation (8000 rpm for 5 min at 4 ˚C) and resuspended in phosphate buffer (PBS). The cells were lysed by supersonic treatment in an ice water bath and then centrifuged (8000 rpm for 20 min at 4 ˚C). The ScDb was re-suspended in PBS containing carbamide (8 mol/L).

The soluble ScDb was purified by a nickel-nitrilotriacetic acid (Ni-NTA) column (Kangweishiji Bio Inc., China) and confirmed by western blot analysis of the His-tag. The diabody was eluted using 100 mM imidazole/PBS and 200 mM imidazole/PBS buffers. SDS–PAGE and western blot analyses with an anti-His-tag antibody were performed to detect and confirm the size and purity of the ScDb-containing fractions. Purified proteins were concentrated in PBS by ultrafiltration with a Centriprep (30 K). The endotoxin was removed by Endotoxin Removal Resin (Thermo, USA) according to the protocol given by the reagent supplier. The endotoxin level of CD40 × HER2 ScDb was evaluated semiquantitatively using a Tachypleus amebocyte lysate (TAL) kit (Zeye Biological, China). The concentration of ScDb were detected by BCA Protein Assay Kit according to the protocol given by the reagent supplier (Beyotime, China).

2.5. Immune activation detection of CD40 × HER2 ScDb

Bone marrow dendritic cells (BMDCs) were isolated from mouse femur and induced in complete DMEM supplemented with 10% fetal calf serum (FCS), granulocyte-macrophage colony-stimulating factor (GM-CSF) (20 ng/mL) (PeproTech, USA) and interleukin-4 (IL-4) (10 ng/mL) (PeproTech, USA) at 37 ˚C in a 5% CO_2 humidified atmosphere. After 4 days of culture, 4T1 frozen-thawed antigen (Ag) (25 μg/mL) was added to the supernatant. After another 2 days of culture, CD40 × HER2 ScDb (300 ng/mL), TNF-α (500 U/mL) (PeproTech, USA) and normal saline (NS) were added to the supernatant after 2 days of incubation.

After all incubations were completed, CD80, CD86 and MHC-II

Table 1
Oligonucleotide sequences of PCR primers in construction of CD40 × HER2 ScDb.

Primer No.	Primer Name	Sequence (5'–3')
P1	Nde I-CD40VH back	5'-CAT ATG GTC CAG CTG CAG CAG TCT GGT-3'
P2	Linker1-CD40VH for	5'-GCT GCC TCC GCC ACC TGA GGA GAC GGT GAC CGT GGT CCC TGG-3'
P3	Linker2-CD40VLback	5'-GAC ATT GAG CTC ACC CAG TCT CCA-3'
P4	Sal I-CD40VL for	5'-GTC GAC CCG TTT TAT TTC CAG CTT GGT CCC-3'
P5	Linker1-HER2VLback	5'-GGT GGC GGA GGC AGC GCA GAT ATT CAG ATG ACT-3'
P6	Linker2-HER2VH for	5'-AGA CCC ACC ACC GCC GGA GCC TCC CCC ACC ACT-3'

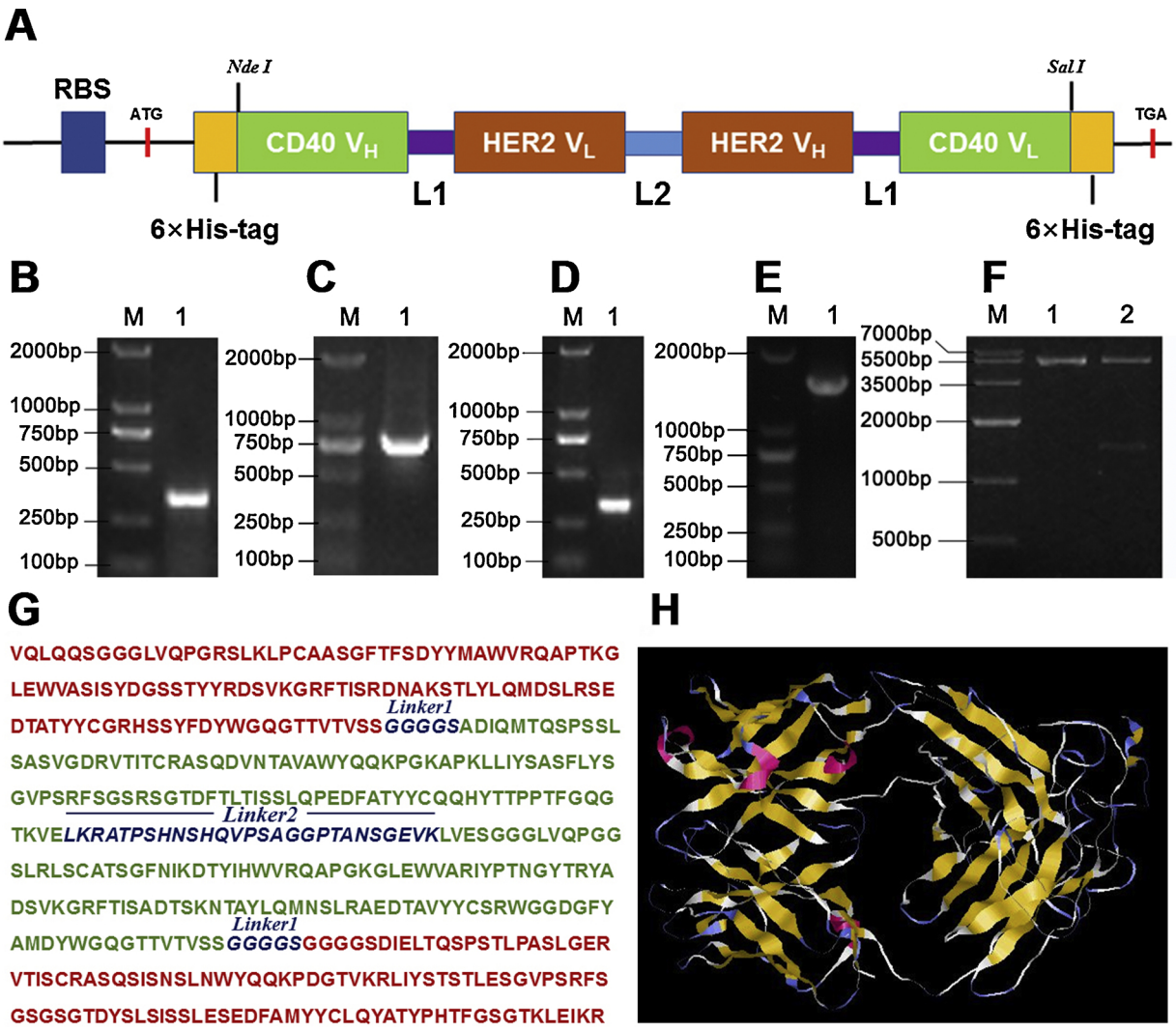

Fig. 1. Construction and structural analysis of CD40 × HER2 ScDb.
A) Molecule structure of ScDb; B). 1: CD40 VH fragment M: Marker DM2000; C). 1: HER2 ScFv M: Marker DM2000; D). 1. CD40 VL fragment M: Marker DM2000 E). 1: CD40 × HER2 ScDb M: Marker DM2000; F). 1: Single restriction analysis of pET28a-ScDb by *Nde I* 2: Double restriction analysis of pET28a -ScDb by *Nde I* and *Sal I*. M: Marker IV; G). Full length sequence of CD40 × HER2 ScDb which included 492 amino acids. H). Tertiary structure prediction of CD40 × HER2 ScDb by I-TASSER.

expression of DCs was estimated by flow cytometry assays. IL-12 expression in different groups was detected by ELISA.

Magnetic column (Miltenyi Biotec USA) purification was used to purify splenic CD3 + T lymphocytes. The proliferation of T lymphocytes in different groups was detected by the CCK-8 test (Dojindo, Japan). IFN-γ expression was estimated by ELISAs. Then, 4T1 cells were cultured and incubated together with T lymphocytes in different groups. The CCK-8 test was applied to evaluate the inhibition rate of 4T1 cells.

For tumor generation, 1×10^6 4T1cells in 100 μL PBS were injected in BALB/c mice subcutaneously in the hind flank. After the tumor models were confirmed, mice were randomly divided into 3 groups (n = 5 for the CD40 × HER2 ScDb group, CD40 mAb group and NS group). Mice received CD40 × HER2 ScDb (1.5 mg/kg), CD40 mAb (5 mg/kg) or NS. The treatment started from the first day when tumor establishment was confirmed (D5) and continued on D8, D11, D14, D17, D20, and D23. Tumor volumes were calculated in cm3 as $0.5 \times (\text{length})^3 \times (\text{width})^2$ after each treatment. After 7 treatments, the mice were sacrificed on D26, and the tumors were harvested and processed for histological staining. Caspase-3 expression was evaluated by immunohistochemistry (IHC), as described in Qiu's study (Qiu et al., 2015).

2.6. HER2 target function evaluation of CD40 × HER2 ScDb

The CD40 × HER2 ScDb was labeled using quantum dots. The quantum dots can exhibit red fluorescence under a 495 nm wavelength excitation. A cellular immunofluorescence assay was applied to evaluate the affinity for HER2. CCK-8 was used to evaluate the inhibition of T6-17 by CD40 × HER2 ScDb. T6-17 cells were divided into aliquots (4000–5000 cells/well), added to 96-well flat-bottom plates and treated with CD40 ScFv (2.5 μg/mL), HER2 ScFv (2.5 μg/mL), CD40 × HER2 ScDb (5 μg/mL), trastuzumab (15 μg/mL) (Roche) or NS. Optical density (OD) values were measured at 570 nm using an ELISA reader. The proliferation inhibition ratio of each group was calculated as follows: Proliferation inhibition ratio (%) = (experimental group OD/negative control group OD) × 100%.

The phosphorylation and expression level of the signal transduction proteins AKT/MEK/ERK in the PI3K/AKT and MAPK/ERK1/2 signal pathways were evaluated by western blot analyses.

To induce tumors, we suspended 5×10^4 T6-17 cells in 100 μL of PBS and injected them subcutaneously into the flank of BALB/c-nude

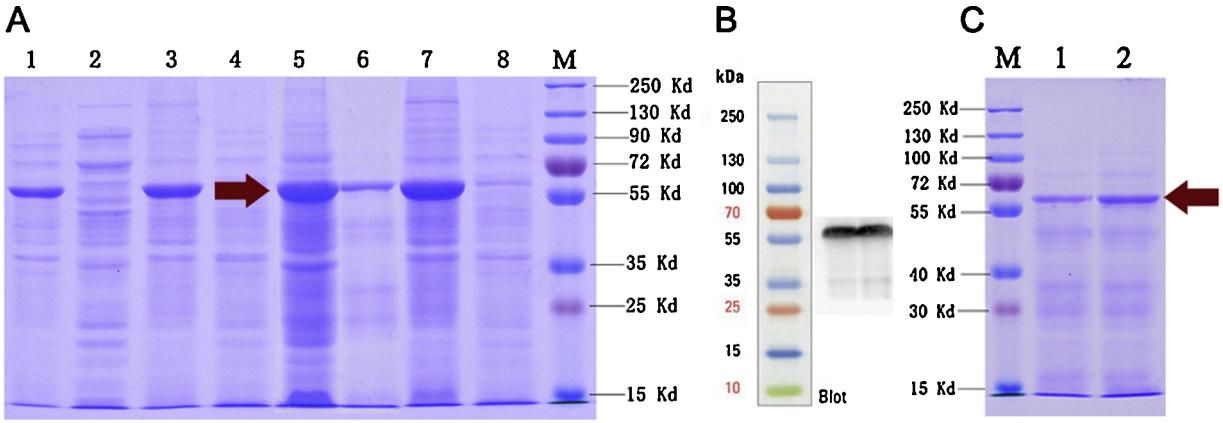

Fig. 2. Expression and purification of CD40 × HER2 ScDb.
A). The expression of ScDb was induced by gradient concentration of IPTG, bacterial lysate supernatant and sediment were detected by SDS-PAGE, 1: Bacterial lysate supernatant induced by 0.1 mM IPTG, 2: Inclusion body induced by 0.1 mM IPTG, 3: Bacterial lysate supernatant induced by 0.2 mM IPTG, 4: Inclusion body induced by 0.2 mM IPTG; 5: Bacterial lysate supernatant induced by 0.5 mM IPTG, 6: Inclusion body induced by 0.5 mM IPTG,7: Bacterial lysate supernatant induced by 1 Mm IPTG, 8: Inclusion body induced by 1 mM IPTG; M: Protein ladder(10–250 kDa); B). His-tag labeled protein was detected by Western blot, Positive protein bands emerge around 55 kDa which was consisted with the expected molecular weight(56.548 kDa) ; C).ScDb induced by IPTG was purified by Ni-NTA, and eluented by gradient concentration of imidazole1: Eluent of 50 mM imidazole; 2: Eluent of 100 mM imidazole; M: Protein ladder(10–250 kDa).

mice. Mice were randomly divided into 5 groups (n = 5 for the CD40 ScFv, HER2 ScFv, CD40 × HER2 ScDb, trastuzumab and NS groups). Mice received CD40 ScFv (150 μg/kg), HER2 ScFv (150 μg/kg), CD40 × HER2 ScDb (300 μg/kg), trastuzumab (1 mg/kg) and NS. The treatment started from the first day when tumor establishment was confirmed (D4) and continued at D8, D12, and D16. Tumor size was determined by Vernier caliper measurements. Tumor volume was calculated as previously described. After 4 treatments, the mice were sacrificed on D20, and the tumors were harvested and processed for histological staining.

2.7. Statistical analysis

The results are presented as the mean ± SD of at least three separate experiments and were analyzed by *t*-test or one-way ANOVA followed by Student-Newman-Keuls multiple comparison tests using PRISM software (GraphPad Software, Inc., San Diego, CA, USA). Significant differences were defined as $P < 0.05$.

3. Results

3.1. Construction and structural analysis of CD40 × HER2 ScDb

The ScDb fragment was constructed as depicted in Fig. 1. The CD40VH, CD40VL, and HER2ScFv domains were amplified by PCR from the pCANTAB5E vector encoding CD40-scFv and the pUC57 vector encoding HER2-ScFv. After purification, CD40VL, HER2ScFv and CD40VH were successively assembled by SOE-PCR to generate ScDb (1464 bp) (Fig. 1D) with a flexible linker (Gly4Ser). The recombinant plasmid pET28a (+)-ScDb was identified by PCR, restriction enzyme digestion, and electrophoretic analysis. A 1500 bp DNA fragment was generated after PCR amplification using pET28a (+)-ScDb as a template (Fig. 1E), and a double digestion (*NdeI* and *SalI*) produced two DNA electrophoretic bands of 1464 bp and 5369 bp (Fig. 1E). The DNA sequencing of the plasmid pET28a(+)-ScDb also confirmed that the inserted DNA fragment was consistent with the ScDb gene. All results showed that the expression vector pET28a(+)-ScDb was successfully constructed.

Based on the sequencing results, a molecular model of CD40 × HER2 ScDb was generated by Protean software: CD40 × HER2 ScDb was translated to 492 amino acids with no frameshifts or deletions (Fig. 1F). The flexible linker (Gly4Ser) was also translated correctly. The tertiary structure of CD40 × HER2 ScDb was imitated by I-TASSER (http://zhanglab.ccmb.med.umich.edu/I-TASSER) (Fig. 1G). The C-score of the model was −1.58, and the estimated TM-score was 0.52 ± 0.15.

3.2. Expression and purification of CD40 × HER2 ScDb

0.5 mM IPTG was used to induce ScDb expression in E. coli Rosetta, which led to a high total amount of expressed soluble ScDb. For the induction time and temperature, 37 °C and 180 rpm for 4 h were identified as the optimal induction conditions (Fig. 2A). Expression of 6His-tagged ScDb in *E.coli* Rosetta (DE3) host strains was identified by SDS-PAGE and western blotting (Fig. 2A and B). The molecular weight of the expressed recombinant protein was expected to be 60 kDa (Fig. 2B). Then, Protein was purified by Ni-NTA, and 100 mM imidazole exhibited the best eluting effect (Fig. 2C). The endotoxin level of prepared protein was assayed using the TAL kit and found to be lower than 0.46 EU/mL. The concentration of purified ScDb was 2.7 mg/mL.

3.3. CD40 × HER2 ScDb inhibited 4T1 cell proliferation via immune activation

Mice BMDCs were stimulated by 4T1 frozen-thawed antigen and CD40 × HER2ScDb in succession and then analyzed by flow cytometry. The results showed a prominent increase in the expression of the DC-activation markers CD80, CD86 and MHC-II (Fig. 3A–C). Furthermore, a notable increase in IL-12p70 expression was detected by ELISA (Fig. 3D), which exhibited a similar pattern ($P > 0.05$) in the Ag + TNF-α group. An ELISA of IFN-γ indicated that T cells could be stimulated by mature BMDCs after interference with CD40 × HER2ScDb (Fig. 3E), To compare the indirect growth inhibitory effect of CD40 × HER2ScDb, we performed CCK-8 tests with 4T1 tumor cells as effector cells. Comparable growth inhibitory effects were observed for the CD40 × HER2ScDb and TNF-α groups in 4T1 cells (Fig. 3F).

In the in vivo experiment, all mice in each group developed tumors reliably. The fastest increase in tumor volume was observed in the group receiving NS only. Tumor growth in the CD40 × HER2ScDb-treated group exhibited a statistically significant reduction ($P < 0.05$) compared to that of the NS group, and statistical significance was observed from days 14 to days 26 (Fig. 3G). Notable lymphocyte infiltration could be found in CD40 × HER2ScDb-treated tumor tissue with IHC staining of Caspase-3, indicating that CD40 × HER2ScDb

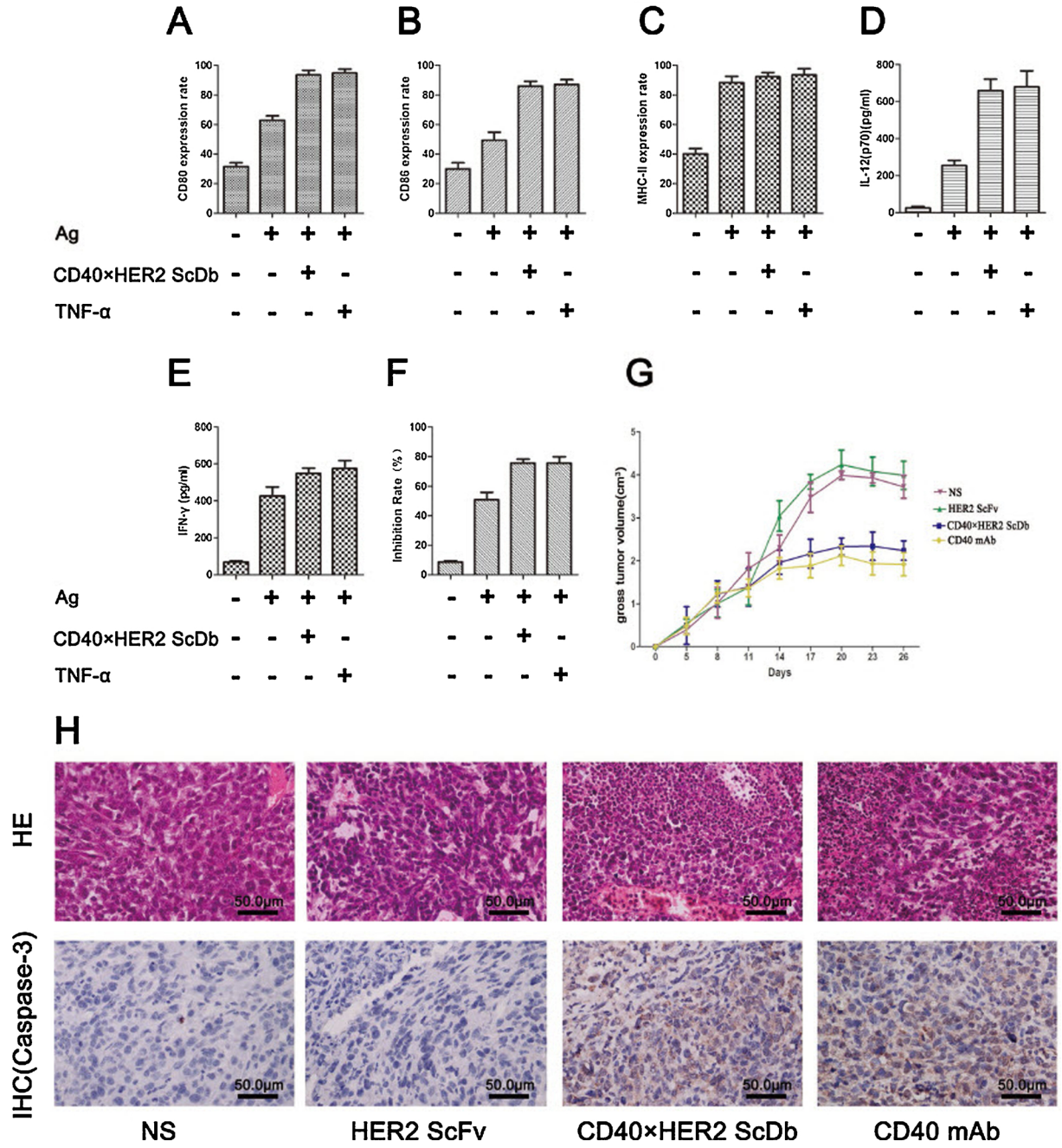

Fig. 3. CD40 × HER2ScDb inhibited 4T1 cell growth in vitro and in vivo.
After all incubations were completed, CD80, CD86 and MHC-II expression of DCs was estimated by flow cytometry assays, the results showed a prominent increase in the expression of the DC-activation markers CD80, CD86 and MHC-II: A). CD80 expression of different groups, B). CD86 expression of different groups, C). MHC-II expression of different groups. IL-12 expression in different groups was detected by ELISA, a notable increase was detected after stimulated by ScDb D). IL-12 p70 expression in different groups, E). IFN-γ expression in different groups. F). Inhibition rate of 4T1 cells in different groups, comparable growth inhibitory effects were observed for the CD40 × HER2ScDb. G). Growth curves of 4T1 cells in BALB/c mice from different groups, tumor growth in the CD40 × HER2ScDb-treated group exhibited a statistically significant reduction. H). Cell morphology and caspase-3 expression in different groups, CD40 × HER2ScDb upregulated Caspase-3 expression, which contributed to the apoptosis and necrosis of 4T1 cells in vivo.

could upregulate Caspase-3 expression, which contributed to the apoptosis and necrosis of 4T1 cells in vivo. However, little lymphocyte infiltration was detected in the NS group (Fig. 3H).

3.4. CD40 × HER2 ScDb inhibited T6-17 cell proliferation via anti-HER2

HER2 target function was confirmed by immunofluorescence assays. The quantum dots can exhibit red fluorescence under a 495 nm wavelength excitation, and the results demonstrated that red fluorescence surrounded the T6-17 cells, which indicated that CD40 × HER2 ScDb could interact with HER2 expressed on the surface of T6-17 cells (Fig. 4A). To investigate whether the beneficial binding of CD40 × HER2ScDb to target-expressing cells results in cytotoxic effects, we performed CCK-8 assays. The results indicated that CD40 × HER2ScDb could dramatically inhibit T6-17 cell proliferation, similar to trastuzumab (Fig. 4B). The results of western blot analysis demonstrated that CD40 × HER2ScDb could competitive inhibit the dimerization of HER2 and block the PI3K/AKT and MAPK/ERK1/2

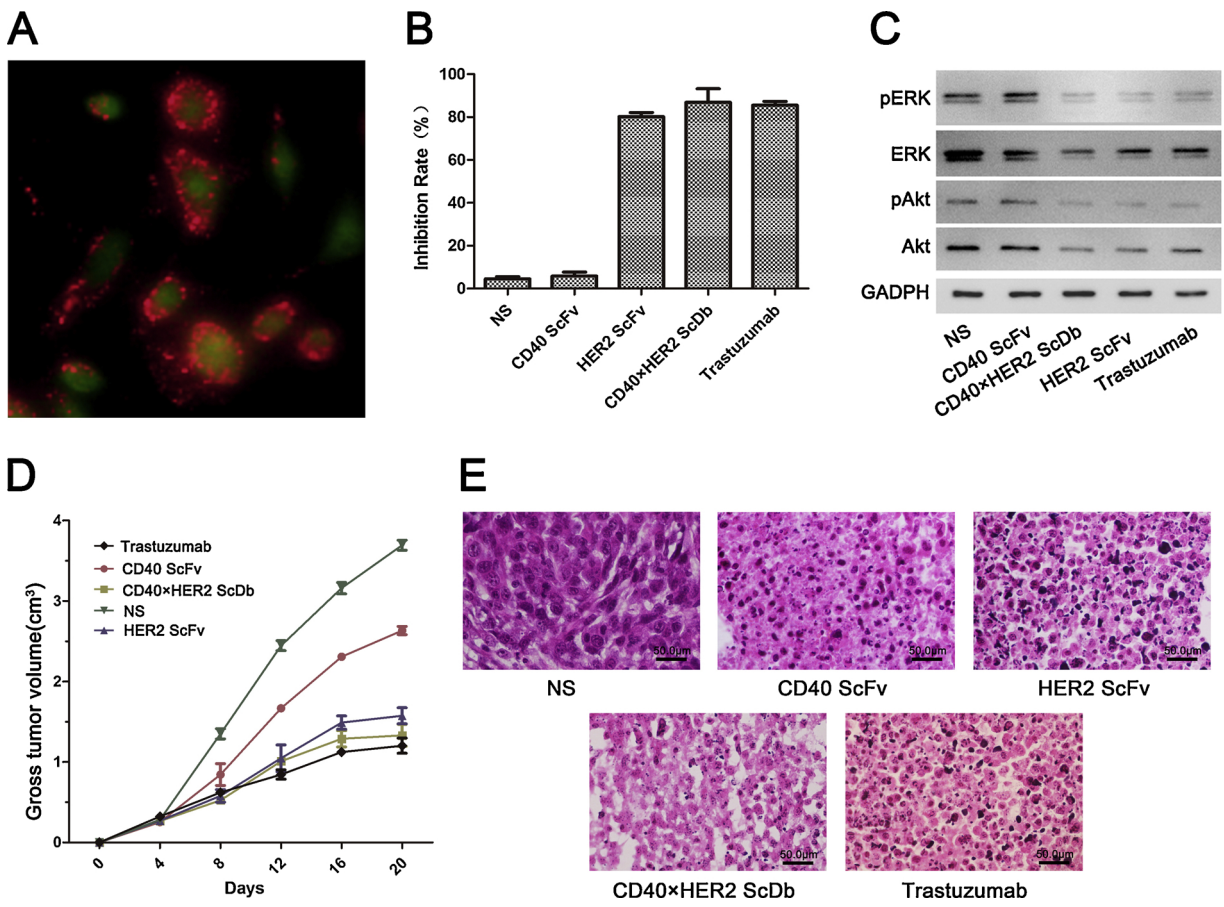

Fig. 4. CD40 × HER2 ScDb inhibited T6-17 cell growth in vitro and vivo by anti-HER2.
A). Immunofluorescence assay results of CD40 × HER2ScDb; red fluorescence representing CD40 × HER2ScDb indicated that the molecule could interact with HER2 expressed on the surface of T6-17. B). Inhibition rate of T6-17 cells in different groups, which indicated that CD40 × HER2ScDb could dramatically inhibit T6-17 cell proliferation. C). The differences in p-Akt and p-ERK between different groups were evaluated by western blot analyses. D). T6-17 growth curve in BALB/c-nude mice from different groups. E). T6-17 cell morphology in different groups was detected by HE staining.

pathways downstream of HER2 (Fig. 4C).

In the in vivo experiment, CD40 × HER2ScDb also substantially inhibited T6-17 growth compared with that of the NS and CD40 ScFv groups ($P < 0.05$), and statistical significance was observed from days 8 to days 20 (Fig. 4D). HE staining of tumor tissues revealed that after CD40 × HER2ScDb treatment, tumor cells showed extensive deformation, and pervasive karyopyknosis and karyorrhexis were found, which was consistent with the shrinkage of tumor volume in the CD40 × HER2ScDb group (Fig.4E).

4. Discussion

The limited options in the treatment of malignancy have encouraged the search for new strategies. One promising approach is the recruitment of cytotoxic immune effector cells to tumor cells by BsAbs or diabodies. Studies have shown that activation of tumor-specific cytotoxic T cells (CTLs) can inhibit tumor proliferation in mouse tumor models (Yan et al., 2015). Therefore, the induction of specific T cell activation against tumors is currently one of the cores of tumor immunotherapy research (Lei et al., 2016). To date, several studies have compared various small BsAb formats, including multimeric formats, and their differences in function; however, no consensus has been established on the most appropriate format (Korn et al., 2004; Kipriyanov et al., 2003; Mølhøj et al., 2007). In the present study, we developed CD40 × HER2 ScDb, a diabody targeting HER2 and CD40, and examined the function of small BsAb formats using cytotoxicity assays, ELISA, western blot, and IHC.

CD40/CD40 L is the main second signal system. Studies have found that tumor cells can inhibit the expression of the second signaling system by expressing several inhibitory immune factors, which contribute to blocking the maturation of DCs and inhibiting the production of effector T cells. Immune tolerance was ultimately induced (Yang et al., 2013). Kosaka (Kosaka et al., 2014) showed that agonistic antibodies against CD40 could bind to CD40 on DCs, promote their maturation and act as CD4+ helper T cells. In a study by Khong (Khong et al., 2013), FGK45 (CD40 mAb) was shown to promote DC cell maturation and induce effector T cell activation by binding to CD40, thereby inhibiting tumor proliferation.

CD80/CD86 belong to the costimulatory adhesion molecule family, which can activate T cells by the costimulatory pathway and have been used as indicators of DC maturation in numerous studies. In addition, MHC-II, as the principal component of antigen presentation, was significantly elevated after antigen loading. Therefore, CD80, CD86 and MHC-II molecules are considered markers of DC maturation (Hunter et al., 2007). IL-12 is one of the most important parameters of DC maturation (Athiemorales et al., 2004). In our research, CD40 × HER2ScDb could significantly upregulate the expression of CD80/CD86/MHC-II compared with that of the NS group and Ag group, and the IL-12 expression of the Ag + CD40 × HER2ScDb group also increased remarkably, which was significantly different from that of the NS group and Ag group. However, there was no significant difference between the Ag + CD40 × HER2ScDb group and Ag + TNF-α group ($P > 0.05$). Our results were consistent with the research of Mangsbo (Mangsbo et al., 2015). Comparable growth inhibitory effects were

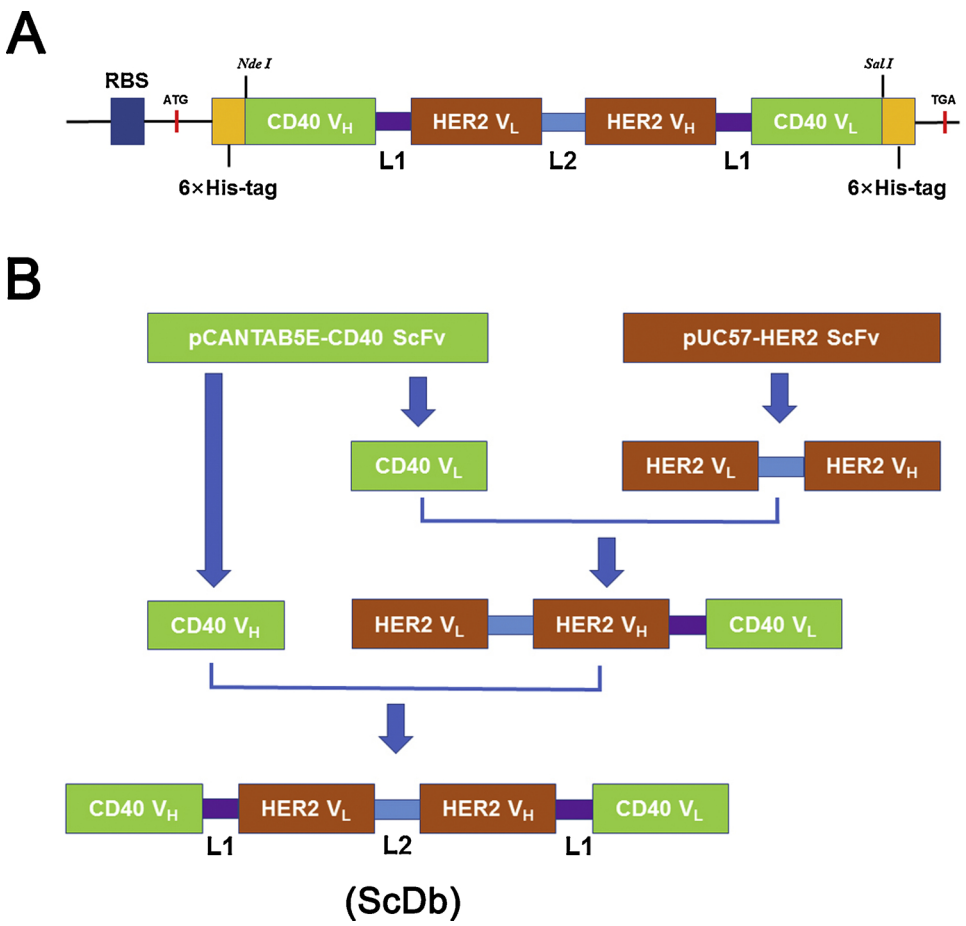

Fig. 5. Diagram of CD40 × HER2 ScDb construction.

observed for the Ag + CD40 × HER2 ScDb and Ag + TNF-α groups in 4T1 cell lines, which indicated that CD40 × HER2ScDb could restrain the proliferation of 4T1 by stimulating tumor-specific immunoreactions. The in vivo murine model studies revealed the remarkable inhibitory effects on T6-17 cells in the CD40 × HER2 ScDb and CD40 mAb groups. Moreover, HE staining demonstrated that CTLs could be assembled in tumor tissues after CD40 × HER2 ScDb was administered. Caspase-3 is a critical protease for activation in the early stage of apoptosis and is the final apoptotic executioner (Liu et al., 1997). In many studies (He et al., 2005; Jerome et al., 2003), Caspase-3 has been used as an indicator of CTL function. In this study, IHC staining of Caspase-3 demonstrated that Caspase-3 was abundantly expressed in the T6-17 cytoplasm after CD40 × HER2 ScDb or CD40 mAb treatment, which indicated that CD40 × HER2 ScDb could induce the apoptosis of 4T1 cells by stimulating CTLs.

HER2 is overexpressed in a wide range of human malignancies, and its expression level is correlated with poor clinical outcome in patients with several cancers, such as breast cancer, gastric cancer and prostate cancer (Roh and Pippin, 2000; Zhang et al., 2009; Liu et al., 2005). Immunofluorescence experiments confirmed that CD40 × HER2 ScDb had a strong affinity for HER2 expressed on the surface of T6-17 cells. The cytotoxicity assays indicated that CD40 × HER2 ScDb could remarkably inhibit the proliferation of T6-17 cells.

Akt is one of the major downstream effectors of PI3K and is phosphorylated after PI3K receives an upstream activation signal. Akt phosphorylation regulates cell proliferation, differentiation, apoptosis and migration by activating or inhibiting its downstream target proteins. Therefore, phosphorylation of Akt is an important indicator of HER2 expression, which affects tumor cell proliferation and metastasis (Shoman et al., 2005). Extracellular signal regulated kinase (ERK) is an important member of the mitogen activated protein kinase (MAPK) family, which plays a vital role in regulating cell proliferation, differentiation, and apoptosis (Eblen et al., 2002). HER2 could activate ERK via MAPK. Activated ERK regulates the function of downstream target genes by phosphorylating transcription factors, cytoskeleton-associated proteins, and other substrates (Eblen et al., 2002). Therefore, the phosphorylation level of ERK can reflect the activation level of the MAPK/ERK signaling pathway. In this study, the expression levels of phosphorylated Akt and ERK in T6-17 cells were detected under different interventions. Western blotting was performed to determine the HER2-targeting mechanism of CD40 × HER2 ScDb. Our experiments showed that CD40 × HER2 ScDb could significantly inhibit the phosphorylation of ERK and Akt compared with that of the NS and CD40 ScFv groups. Therefore, we speculated that CD40 × HER2 ScDb could inhibit the proliferation of tumor cells and promote their apoptosis by inhibiting the PI3K/AKT and MAPK/ERK1/2 signaling pathways. In the present study, we evaluated the function of CD40 × HER2 ScDb in vivo by constructing a T6-17 tumor model in BALB/c-nude mice. By comparing the differences in the tumor growth curves of each group, we found that the CD40 × HER2 ScDb group and the trastuzumab group had inhibited tumor proliferation, and the difference was significant compared with that of the NS group ($P < 0.05$). No significant difference was found between the CD40 × HER2 ScDb group and the trastuzumab group. HE staining of tissue slices indicated that after CD40 × HER2 ScDb was administered, T6-17 cells lost their normal morphology, the chromatin aggregated and the nucleus volume decreased. In some fields, only the blurred nuclear outline or nuclear debris could be found, which indicated that CD40 × HER2 ScDb could induce the apoptosis of T6-17 in vivo by targeting HER2 and blocking the downstream signal pathway.

5. Conclusion

In conclusion, we successfully constructed a CD40 × HER2 ScDb fragment by SOE-PCR and expressed it using a prokaryotic expression system. The in vivo and in vitro experimental results indicated that CD40 × HER2 ScDb could inhibit the proliferation of tumor cells by stimulating tumor-specific immunoreactions and blocking the HER2-related signaling pathway.

Acknowledgments

This research was funded by Tianjin Health Institution Key Projects, grant number 15KG148" and "Tianjin Medical University General Hospital Youth Incubation Fund, grant number ZYYFY2017029". I would like to express my heartfelt gratitude to Professor Hongtao Zhang for his generous gifting of the recombinant pUC57 vector encoding HER2-ScFv.

References

Athiemorales, V., Smits, H.H., Cantrell, D.A., Hilkens, C.M., 2004. Sustained il-12 signaling is required for th1 development. J. Immunol. 172 (1), 61–69.

Bang, Y.J., Van, C.E., Feyereislova, A., Chung, H.C., Shen, L., Sawaki, A., et al., 2010. Trastuzumab in combination with chemotherapy versus chemotherapy alone for treatment of her2-positive advanced gastric or gastro-oesophageal junction cancer (TOGA): a phase 3, open-label, randomised controlled trial. Lancet 376 (9742), 687–697. https://doi.org/10.1016/S0140-6736(10)61121-X.

Begnami, M.D., Fukuda, E., Fregnani, J.H.T.G., Nonogaki, S., Montagnini, A.L., Da Costa, W.L., et al., 2011. Prognostic implications of altered human epidermal growth factor receptors (hers) in gastric carcinomas: her2 and her3 are predictors of poor outcome. J. Clin. Oncology 29 (22), 3030–3036. https://doi.org/10.1200/JCO.2010.33.6313.

Cao, Y., 2003. Bispecific antibody conjugates in therapeutics. Adv. Drug Deliv. Rev. 55 (2), 171–197.

Chawla, A., Alatrash, G., Wu, Y., Mittendorf, E.A., 2013. Immune aspects of the breast tumor microenvironment. Breast Cancer Manag. 2 (3), 231–244. https://doi.org/10.2217/bmt.13.15.

Eblen, S.T., Slack, J.K., Weber, M.J., Catling, A.D., 2002. Rac-pak signaling stimulates extracellular signal-regulated kinase (erk) activation by regulating formation of mek1-erk complexes. Mol. Cell. Biol. 22 (17), 6023.

He, L., Hakimi, J., Salha, D., Miron, I., Dunn, P., Radvanyi, L., 2005. A sensitive flow cytometry-based cytotoxic t-lymphocyte assay through detection of cleaved caspase 3 in target cells. J. Immunol. Methods 304 (1-2), 43–59. https://doi.org/10.4049/jimmunol.1301668.

Hunter, T.B., Alsarraj, M., Gladue, R.P., Bedian, V., Antonia, S.J., 2007. An agonist antibody specific for cd40 induces dendritic cell maturation and promotes autologous anti-tumour t-cell responses in an in vitro mixed autologous tumour cell/lymph node cell model. Scandinavian J. Immunol. 65 (5), 8. https://doi.org/10.1111/j.1365-3083.2007. 01927.x.

Jerome, K.R., Sloan, D.D., Aubert, M., 2003. Measurement of ctl-induced cytotoxicity: the caspase 3 assay. Apoptosis 8 (6), 563–571. https://doi.org/10.1007/s00262-014-1561-8.

Kawashita, Y., Deb, N.J., Garg, M.K., Kabarriti, R., Fan, Z., Alfieri, A.A., et al., 2014. An autologous in situ tumor vaccination approach for hepatocellular carcinoma. 2. Tumor-specific immunity and cure after radio-inducible suicide gene therapy and systemic cd40-ligand and flt3-ligand gene therapy in an orthotopic tumor model. Radiat. Res. 182 (2), 201–210. https://doi.org/10.1667/RR13617.1.

Khong, A., Brown, M.D., Vivian, J.B., Robinson, B.W.S., Currie, A.J., 2013. Agonistic anti-cd40 antibody therapy is effective against postoperative cancer recurrence and metastasis in a murine tumor model. J. Immunother. 36 (7), 365–372. https://doi.org/10.7150/jca.5046.

Kipriyanov, S.M., Moldenhauer, G., Braunagel, M., Reusch, U., Cochlovius, B., Gall, F.L., et al., 2003. Effect of domain order on the activity of bacterially produced bispecific single-chain fv antibodies. J. Mol. Biol. 330 (1), 0–111.

Korn, T., Nettelbeck, D.M., VöLkel, T., Müller, Rolf, Kontermann, R.E., 2004. Recombinant bispecific antibodies for the targeting of adenoviruses to cea-expressing tumour cells: a comparative analysis of bacterially expressed single-chain diabody and tandem scfv. J. Gene Med. 6 (6), 642–651. https://doi.org/10.1002/jgm.555.

Kosaka, A., Ohkuri, T., Okada, H., 2014. Combination of an agonistic anti-cd40 monoclonal antibody and the cox-2 inhibitor celecoxib induces anti-glioma effects by promotion of type-1 immunity in myeloid cells and t-cells. Cancer Immunol. Immunother. 63 (8), 847–857.

Kramer, K., Hock, B., 2003. Recombinant antibodies for environmental analysis. Anal. Bioanal. Chem. 377 (3), 417–426. https://doi.org/10.1007/s00216-003-2161-1.

Kufer, P., Lutterbüse, R., Baeuerle, P.A., 2004. A revival of bispecific antibodies. Trends Biotechnol. 22 (5), 238–244. https://doi.org/10.1016/j.tibtech.2004.03.006.

Lei, J., Wu, Z., Jiang, Z., Li, J., Zong, L., Chen, X., et al., 2016. Pancreatic carcinoma-specific immunotherapy using novel tumor specific cytotoxic t cells. ONCOTARGET. https://doi.org/10.18632/oncotarget.13469.

Liu, X., Zou, H., Slaughter, C., Wang, X., 1997. Dff, a heterodimeric protein that functions downstream of caspase-3 to trigger dna fragmentation during apoptosis. Cell 89 (2), 175–184. https://doi.org/10.4049/jimmunol.1301668.

Mangsbo, S.M., Broos, S., Fletcher, E., Veitonmäki, Niina, Furebring, C., Dahlén, Eva, et al., 2015. The human agonistic cd40 antibody adc-1013 eradicates bladder tumors and generates t cell dependent tumor immunity. Clin. Cancer Res. 21 (5), 1115–1126. https://doi.org/10.1158/1078-0432.CCR-14-0913.

Mølhøj, Michael, Crommer, S., Brischwein, K., Rau, D., Sriskandarajah, M., Hoffmann, P., et al., 2007. Cd19-/cd3-bispecific antibody of the bite class is far superior to tandem diabody with respect to redirected tumor cell lysis. Mol. Immunol. 44 (8), 1935–1943. https://doi.org/10.1016/j.molimm.2006.09.032.

Qiu, X., Klausen, C., Cheng, J.C., Leung, P.C.K., 2015. Cd40 ligand induces rip1-dependent, necroptosis-like cell death in low-grade serous but not serous borderline ovarian tumor cells. Cell Death Dis. 6 (8), e1864. https://doi.org/10.1038/cddis.2015.229.

Roh, H., Pippin, J.J., 2000. Down-regulation of her2/neu expression induces apoptosis in human cancer cells that overexpress her2/neu. Cancer Res. 60 (3), 560–565.

Schrama, D., Reisfeld, R.A., Becker, J.ürgen C., 2006. Antibody targeted drugs as cancer therapeutics. Nat. Rev. Drug Discov. 5 (2), 147–159. https://doi.org/10.1038/nrd1957.

Shoman, N., Klassen, S., Mcfadden, A., Bickis, M.G., Torlakovic, E., Chibbar, R., 2005. Reduced pten expression predicts relapse in patients with breast carcinoma treated by tamoxifen. Modern Pathology An Official Journal of the United States & Canadian Academy of Pathology Inc 16 (3). https://doi.org/10.1038/modpathol.3800296. 250–250.

Singer, C.F., KöStler, W.J., Hudelist, G., 2008. Predicting the efficacy of trastuzumab-based therapy in breast cancer: current standards and future strategies. Biochim. Biophys. Acta 1786 (2), 105–113. https://doi.org/10.1016/j.bbcan.2008.02.003.

Slamon, D.J., Clark, G.M., Wong, S.G., Levin, W.J., Ullrich, A., McGuire, W.L., 1987. Human breast cancer: correlation of relapse and survival with amplification of the HER-2/neu oncogene. Cancer Res. 37 (2), 445–450.

Liu, Y., Majumder, S., Mccall, W., Sartor, C.I., Whang, Y.E., 2005. Inhibition of her-2/neu kinase impairs androgen receptor recruitment to the androgen regulated enhancer. Cancer Res. 65 (8), 3404–3409.

Yan, Y., Li, S., Jia, T., Du, X., Xu, Y., Zhao, Y., et al., 2015. Combined therapy with ctl cells and oncolytic adenovirus expressing il-15-induced enhanced antitumor activity. Tumour Biol. 36 (6), 4535–4543. https://doi.org/10.1007/s13277-015-3098-7.

Yang, M., Shurin, G.V., Zhu, P., Shurin, M.R., 2013. Dendritic cells in the cancer microenvironment. J. Cancer 4 (1), 36–44.

Yau, K.Y.F., Lee, H., Hall, J.C., 2003. Emerging trends in the synthesis and improvement of hapten-specific recombinant antibodies. Biotechnol. Adv. 21 (7), 599–637.

Yokoyama, H., Ikehara, Y., Kodera, Y., Ikehara, S., Yatabe, Y., Mochizuki, Y., et al., 2006. Molecular basis for sensitivity and acquired resistance to gefitinib in her2-over-expressing human gastric cancer cell lines derived from liver metastasis. Br. J. Cancer 95 (11), 1504–1513. https://doi.org/10.1038/sj.bjc.6603459.

Zhang, X.L., Yang, Y.S., Xu, D.P., Qu, J.H., Guo, M.Z., Gong, Y., et al., 2009. Comparative study on overexpression of her2/neu and her3 in gastric cancer. World J. Surg. 33 (10), 2112. https://doi.org/10.1007/s00268-009-0142-z.